Maturation of Human Embryonic Stem Cell–Derived Pancreatic Progenitors Into Functional Islets Capable of Treating Pre-existing Diabetes in Mice

Alireza Rezania,[1] Jennifer E. Bruin,[2] Michael J. Riedel,[2] Majid Mojibian,[2] Ali Asadi,[2] Jean Xu,[1] Rebecca Gauvin,[1] Kavitha Narayan,[1] Francis Karanu,[1] John J. O'Neil,[1] Ziliang Ao,[3] Garth L. Warnock,[3] and Timothy J. Kieffer[2,3]

Diabetes is a chronic debilitating disease that results from insufficient production of insulin from pancreatic β-cells. Islet cell replacement can effectively treat diabetes but is currently severely limited by the reliance upon cadaveric donor tissue. We have developed a protocol to efficiently differentiate commercially available human embryonic stem cells (hESCs) in vitro into a highly enriched PDX1+ pancreatic progenitor cell population that further develops in vivo to mature pancreatic endocrine cells. Immature pancreatic precursor cells were transplanted into immunodeficient mice with streptozotocin-induced diabetes, and glycemia was initially controlled with exogenous insulin. As graft-derived insulin levels increased over time, diabetic mice were weaned from exogenous insulin and human C-peptide secretion was eventually regulated by meal and glucose challenges. Similar differentiation of pancreatic precursor cells was observed after transplant in immunodeficient rats. Throughout the in vivo maturation period hESC-derived endocrine cells exhibited gene and protein expression profiles that were remarkably similar to the developing human fetal pancreas. Our findings support the feasibility of using differentiated hESCs as an alternative to cadaveric islets for treating patients with diabetes. ***Diabetes*** **61:2016–2029, 2012**

Patients with diabetes are characterized by an absolute or relative lack of insulin-secreting pancreatic β-cells, resulting in an inability to normalize blood glucose levels (1). Clinical islet transplantation is an effective therapy for diabetes, producing sustained insulin independence or reduced insulin requirements in most patients (2,3). Unfortunately, because of the scarceness of cadaveric islet donors, widespread adoption of this therapy is impractical. Human embryonic stem cells (hESCs) are a promising alternative cell source for treating diabetes, and numerous groups have generated insulin-producing cells in vitro using stepwise differentiation protocols that mimic pancreatic development (4–13). However, our knowledge of pancreas development is inevitably based on model organisms (14–17), and consequently, there are gaps in our understanding of human pancreas development. As such, the field continues to struggle with the production of mature insulin–producing cells that respond to appropriate secretagogues and possess all hallmarks of true adult human β-cells. For instance, most in vitro stepwise differentiation protocols produce pancreatic endocrine cells that coexpress glucagon and insulin, suggestive of an immature cell type (5,8,9,18).

An alternative strategy for promoting β-cell maturation is transplantation of hESC-derived pancreatic progenitor cells, thus allowing maturation to occur in vivo. Grafts of human fetal islet–like cell clusters successfully matured into glucose-responsive insulin-producing cells in mice (19), suggesting that a similar approach may be feasible for hESC-derived cells. Although early studies using this approach reported amelioration of streptozotocin (STZ)-induced hyperglycemia following transplantation of hESC-derived cells, circulating human C-peptide was either not measured (12) or too low to be clinically relevant (6). Furthermore, although C-peptide–positive cells were detected in the kidney grafts, these were not mature β-cells, since they expressed multiple hormones (12) and did not uniformly express crucial markers of mature β-cells (6,12). ViaCyte (formerly Novocell) was the first to provide convincing evidence of β-cell maturity in vivo, with glucose-responsive C-peptide secretion and monohormonal insulin-positive cells that coexpressed PDX1, NKX6.1, MAFA, C-peptide, and prohormone processing enzymes (10). This study and a recent follow-up (4) represented important advances for the field, but also raised questions about the clinical applicability of transplanting a mixed population of immature hESC-derived cells. First, ~15–45% of mice transplanted with pancreatic progenitor cells developed grafts with teratomous elements (4,10). Second, ViaCyte did not demonstrate maturation of hESC-derived cells in a pre-existing diabetic environment, but rather showed that once mature, their cells prevented STZ-induced hyperglycemia, a scenario that would not occur clinically (10). Others have attempted to repeat the D'Amour protocol (9) with different cell lines and either failed to generate pancreatic endocrine cells (11) or generated insulin-positive cells at very low efficiency (8). This is likely a reflection of the variability between hESC lines (8,9,11,20), and given the limited access to the CYT49 line, it has been challenging to reproduce their findings. In addition, the in vivo development of pancreatic progenitor cells could not be replicated in nude rats; only rare islet-like

From the [1]BetaLogics Venture, Janssen Research and Development, LLC, Raritan, New Jersey; the [2]Laboratory of Molecular and Cellular Medicine, Department of Cellular and Physiological Sciences, Life Sciences Institute, University of British Columbia, Vancouver, British Columbia, Canada; and the [3]Department of Surgery, University of British Columbia, Vancouver, British Columbia, Canada.

Corresponding author: Timothy J. Kieffer, tim.kieffer@ubc.ca, or Alireza Rezania, arezani@its.jnj.com.

Received 23 January 2012 and accepted 19 May 2012.

DOI: 10.2337/db11-1711

This article contains Supplementary Data online at http://diabetes.diabetesjournals.org/lookup/suppl/doi:10.2337/db11-1711/-/DC1.

A.R. and J.E.B. contributed equally to this work.

M.J.R. is currently affiliated with STEMCELL Technologies, Vancouver, British Columbia, Canada.

endocrine cells developed and circulating human C-peptide was either undetectable or clinically insufficient and not glucose regulated (21).

Here we describe a novel 14-day, four-stage differentiation protocol that generates immature pancreatic endoderm cells in vitro with commercially available H1 cells, one of the most commonly used hESC lines (22). H1 cells were directed, without cell sorting, into a highly enriched PDX1+ pancreatic progenitor population that generated mature islet-like cells in mice with pre-existing diabetes; exogenous insulin therapy was used until the engrafted cells produced sufficient insulin to maintain normoglycemia. The maturation of hESCs was robustly characterized in vitro and in vivo and found to reproducibly mimic human fetal pancreas development.

RESEARCH DESIGN AND METHODS

In vitro differentiation of hESCs. The H1 hESC line was obtained from WiCell Research Institute (Madison, WI) and ESI-49 cells (23) from BioTime (Alameda, CA); hESCs were cultured as previously described (18). Experiments with H1 cells performed at University of British Columbia (UBC) were approved by the Canadian Stem Cell Oversight Committee and UBC Clinical Research Ethics Board. Cells were directed through key stages of pancreatic development, including definitive endoderm (stage 1), primitive gut tube (stage 2), posterior foregut (stage 3), and pancreatic endoderm and endocrine precursors (stage 4). Refer to the Supplementary Data online for detailed methods describing the protocol optimization. The following is the final protocol developed for H1 cells (summarized in Fig. 2*A*).

Stage 1: Definitive endoderm (3 days). Confluent adherent cultures (60–70%) of undifferentiated H1 cells plated on 1:30 Matrigel–coated surfaces were exposed to RPMI 1640 medium (Invitrogen) supplemented with 0.2% FBS (Hyclone), 100 ng/mL activin-A (Pepro-tech; Rocky Hill, NJ), and 20 ng/mL Wnt3A (R&D Systems) for day 1 only. For the next 2 days cells were cultured in RPMI 1640 medium with 0.5% FBS and 100 ng/mL activin-A.

Stage 2: Primitive gut tube (3 days). Stage 1 cells were exposed to Dulbecco's modified Eagle's medium (DMEM)-F12 medium (Invitrogen) supplemented with 2% FBS and 50 ng/mL FGF7 (Pepro-tech) for 3 days.

Stage 3: Posterior foregut (4 days). Cultures were continued for 4 days in DMEM-HG medium (Invitrogen) supplemented with 0.25 μmol/L SANT-1 (Sigma-Aldrich, St. Louis, MO), 2 μmol/L retinoic acid (Sigma-Aldrich), 100 ng/mL Noggin (R&D Systems), and 1% (vol/vol) B27 (Invitrogen).

Stage 4: Pancreatic endoderm and endocrine precursors (4 to 5 days). Stage 3 cells were cultured for 3 to 4 days in DMEM-high glucose (HG) medium supplemented with 1 μmol/L ALK5 inhibitor II (ALK5i; Axxora, San Diego, CA), 100 ng/mL Noggin, 50 nmol/L TPB ((2S,5S)-(*E*,*E*)-8-(5-(4-(trifluoromethyl) phenyl)-2,4-pentadienoylamino)benzolactam; EMD Chemicals, Gibbstown, NJ), and 1% B27 in monolayer format. For the last day of culture, cells were treated with 5 mg/mL dispase for 5 min, followed by gentle pipetting to break into cell clumps (<100 micron). Cell clusters were transferred into polystyrene 125 mL Spinner Flask (Corning) and spun at 80–100 rpm overnight in suspension with DMEM-HG supplemented with 1 μmol/L ALK5i, 100 ng/mL Noggin, and 1% B27.

Flow cytometry. hESC-derived cells were released into single-cell suspension and either stained directly for surface markers or fixed and stained for various intracellular markers. Refer to the Supplementary Data online for additional details.

High content image analysis. For quantitative analysis of intracellular protein expression, cells in 6-well culture plates were fixed and stained with various antibodies (Supplementary Table 2). Refer to the Supplementary Data online for additional details.

Quantitative RT-PCR. Gene expression was analyzed throughout the in vitro differentiation and at 34 weeks posttransplant. Quantitative RT-PCR was performed with custom TaqMan Arrays for cultured cells (primers in Supplementary Table 3; Applied Biosystems, Foster City, CA) and with custom-designed SA Biosciences arrays for engrafted cells (primers in Supplementary Table 4; SA Biosciences, Frederick, MD). Refer to the Supplementary Data online for additional details.

Animal studies and transplantation of hESC-derived cells or human islets. All experiments were approved by the UBC Animal Care Committee. Male 8- to 10-week-old SCID-beige mice (C.B-*Igh*-1b/GbmsTac-*Prkdc*^{scid}-*Lyst*^{bg}N7; Taconic, Hudson, NY) were maintained on a 12-h light/dark cycle with ad libitum access to a standard irradiated diet (Harlan Laboratories, Teklad Diet No. 2918; Madison, WI). Blood glucose and body weight were monitored weekly following a 4-h morning fast. Blood glucose was measured via the saphenous vein using a handheld glucometer (LifeScan; Burnaby, BC, Canada). Three independent cohorts of mice were transplanted; cohorts 1 and 2 were conducted at UBC (Vancouver, BC, Canada) and cohort 3 at the Janssen vivarium facility (Raritan, NJ). In cohorts 1 and 2, mice were rendered diabetic with a single intraperitoneal injection of STZ (cohort 1: 175 mg/kg, n = 6; cohort 2: 190 mg/kg, n = 16). In cohort 1, a subset of mice (n = 3) was retained as nondiabetic controls (no STZ) and all mice in cohort 3 (n = 5) were nondiabetic. In diabetic animals, a slow-release insulin pellet (LinBit; Linshin Canada; Toronto, ON, Canada) was implanted subcutaneously and replaced as needed to control glucose levels.

Mice were anesthetized with inhalable isoflurane and received transplants of 3 to 4 million (cohorts 1 and 2) or 5 million (cohort 3) stage 4 hESC-derived cells under the left kidney capsule. After transplantation all mice were treated with oral enrofloxacin (Bayer Animal Health; Shawnee Mission, KS) for 1 week (100 μg/mL in drinking water). Two cohorts of 6-week-old nondiabetic immunodeficient (nude) male rats (Crl:NIH-*Foxn1*^{rnu}; Charles River Laboratories, Wilmington, MA) were transplanted with 7 million cells under the kidney capsule (n = 5/cohort) to examine cell maturation in a different species. Human islets were obtained from the Irving K. Barber Human Islet Isolation Laboratory (Vancouver, BC, Canada) and ~3,000–4,000 islet equivalents were transplanted under the kidney capsule of nondiabetic (no STZ) SCID-beige mice (n = 3).

Analysis of transplanted cells. All metabolic analyses were performed in conscious, restrained animals on the indicated days. Refer to the Supplementary Data online for detailed procedures.

Engrafted kidneys were fixed in 4% paraformaldehyde for subsequent immunohistochemistry from mice in cohort 1 at 34 weeks; cohort 2 at 4 (n = 4), 12 (n = 4), or 34 (n = 5) weeks; cohort 3 at 17 weeks (n = 2); and nude rats in cohort 2 at 16 weeks posttransplant (n = 1). A piece of engrafted tissue was dissected from mice at 34 weeks and stored in RNAlater (n = 3) or 2% glutaraldehyde (Sigma-Aldrich) for electron microscopy (n = 1).

Immunohistochemistry. Stage 4 pretransplant clusters and engrafted kidneys were fixed in 4% paraformaldehyde. Clusters were embedded in 1% agarose and then all tissues stored in 70% EtOH before paraffin embedding and sectioning (Wax-it Histology Services; Vancouver, BC, Canada).

Hematoxylin-eosin staining was performed using a standard protocol, and slides were scanned with the ScanScope CS system (Aperio; Vista, CA); all grafts were examined by an independent pathologist. Immunofluorescent staining was performed as previously described (18); primary antibodies are detailed in Supplementary Table 5. Images were captured using the ImageXpress Micro Imaging System and analyzed with MetaXpress Software (Molecular Devices Corporation, Sunnyvale, CA); the same acquisition time was used when comparing engrafted cells to human pancreas. Refer to the Supplementary Data online for a description of image quantification.

Electron microscopy. Engrafted cells stored in 2% glutaraldehyde were processed as previously described (24), with the exception that Spurr's epoxy resin was used instead of epon/araldite resin (Canemco, Montreal, QC, Canada). Grids were examined with a Hitachi H7600 Transmission Electron Microscope (TEM; Hitachi High Technologies Corporation, Tokyo, Japan), and representative images were captured with a side mount AMT Advantage (1 megapixel) charged-coupled device camera (Hamamatsu ORCA; Hamamatsu Corporation, Bridgewater, NJ).

Statistical analysis. All statistics were performed using GraphPad Prism software (GraphPad Software, La Jolla, CA). Refer to the Supplementary Data online for details.

RESULTS

Optimization of in vitro differentiation protocol. The differentiation protocol was optimized to direct H1 hESCs through four key stages of pancreatic development (Fig. 2*A*), building on published protocols (9,10,18). We first evaluated the capacity for H1 cells to form pancreatic endocrine progenitors following differentiation with various medias, each containing >40 components that could alter pancreatic endoderm/endocrine formation (Supplementary Fig. 1). DMEM-F12 showed the greatest induction of *NGN3*, *PDX1*, and *NEUROD1* expression, but also inhibited *NKX6.1*. DMEM-HG was the only formulation that did not inhibit *NKX6.1* and also minimized expression of *CDX2* (intestinal lineage; Supplementary Fig. 1). Gap analysis identified the concentration of nonessential amino acids, fatty acids, and HEPES as major differences between DMEM-HG and other formulations; the role of HEPES was

further investigated. Addition of even a low concentration of HEPES (5 mmol/L) to the stage 4 DMEM-HG media dramatically inhibited gene expression of pancreatic lineage markers and promoted development of the intestinal lineage (Fig. 1*A*).

We next modified additional components of the stage 4 medium to further enhance the progenitor population. Chen and colleagues (25) previously demonstrated that protein kinase C (PKC) agonists enhanced PDX1 expression, particularly during later stages of hESC differentiation. We tested two PKC activators, TPB and PBDu (26), in stage 4 media with and without ALK5i/Noggin. *NKX6.1* expression increased approximately fourfold in stage 4 (relative to stage 3) with ALK5i/Noggin alone, whereas a ~50-fold induction was observed when TPB or PBDu was included during stage 4 (Fig. 1*B*). Furthermore, the combination of ALK5i/Noggin/PKC activator resulted in a greater induction of *NGN3*, *NEUROD1*, and *PTF1a*; maintenance of high *PDX1*; and minimal expression of intestinal and liver markers relative to ALK5i/Noggin alone (Fig. 1*B*). TPB >60 nmol/L caused downregulation of proendocrine transcription factors (Fig. 1*C*), as opposed to the induction observed with lower concentrations (Fig. 1*B* and *C*). Therefore, for subsequent studies 50 nmol/L TPB was included during stage 4 (TPB was selected over PBDu for its safer profile [26]).

It is noteworthy that the addition of the three factors (ALK5i/Noggin/TPB) during stage 4 reduced formation of nonpancreatic lineages in vitro (Fig. 1*F*) and prevented overgrowth of engrafted cells in vivo (Fig. 1*H*). Cells differentiated without ALK5i/Noggin/TPB generated high circulating levels of human C-peptide by 16 weeks post-transplant (Fig. 1*G*), but also developed overgrown grafts containing fluid-filled cysts (Fig. 1*H*; 60% of mice [3 of 5] had grafts >20 mm when cells were differentiated in basal stage 4 media; no mice [0 of 4] had grafts >20 mm after

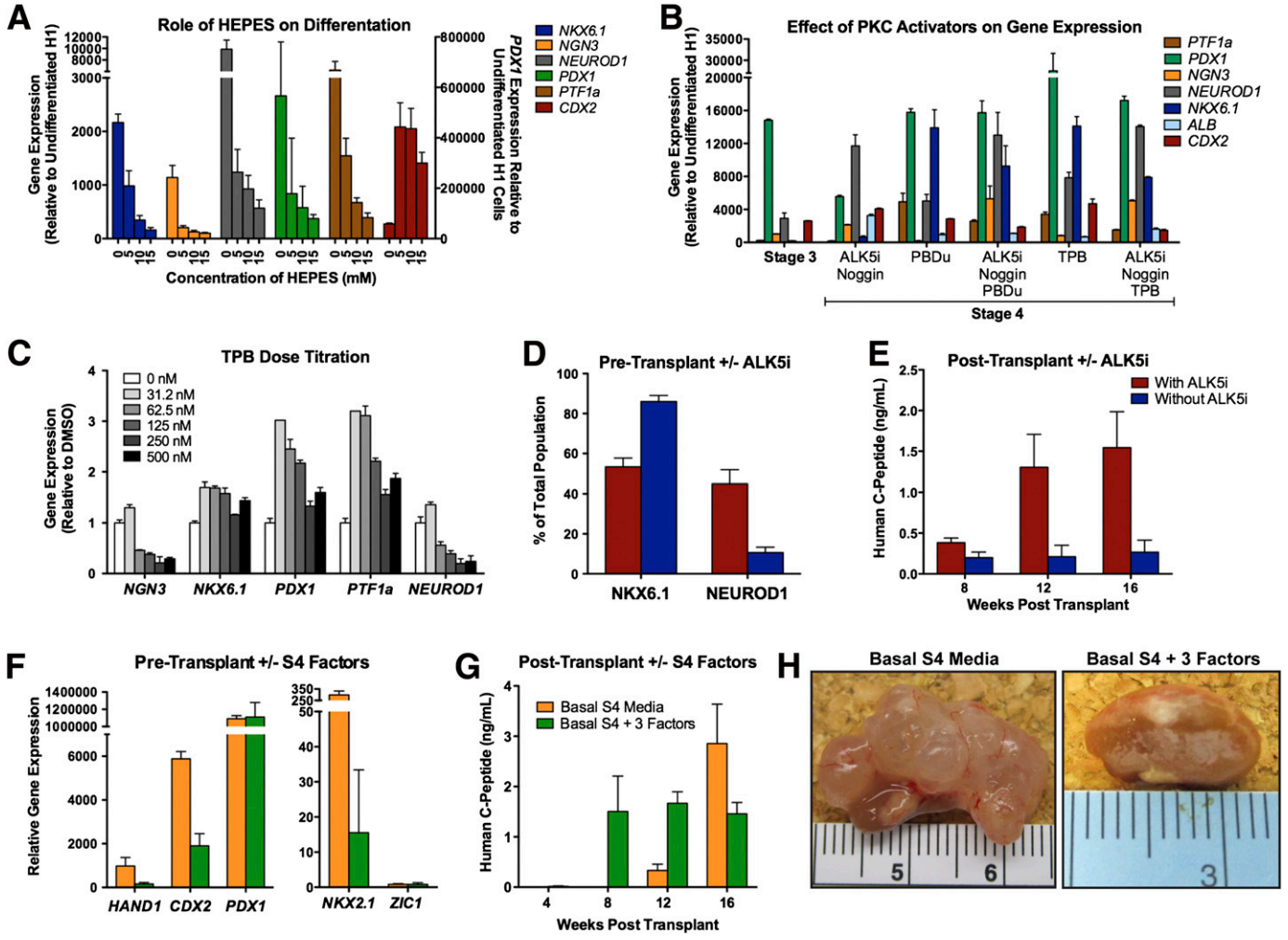

FIG. 1. Optimization of the in vitro differentiation protocol. *A–C*: The effect of various stage 4 (S4) formulations on gene expression of pancreatic endocrine (*PDX1*, *PTF1a*, *NEUROD1*, *NKX6.1*, and *NGN3*), intestinal (*CDX2*), and hepatic (*ALB*) lineage markers. Specifically, the following conditions were examined: addition of HEPES to DMEM-HG S4 medium (*A*); various combinations of ALK5i, Noggin, and/or protein kinase C (PKC) activators, PBDu or TPB, during S4 (*B*); and different TPB concentrations during S4 (*C*). *D*: Removal of ALK5i during S4 resulted in more NKX6.1-positive cells, but fewer NeuroD1-positive cells, as determined by fluorescence-activated cell sorter (FACS) quantification. *E*: Human C-peptide levels (ng/mL) at 8, 12, and 16 weeks following transplantation of cells differentiated with and without ALK5i during S4 (i.e., ALK5i/TPB/Noggin vs. TPB/Noggin). *F–H*: When compared with basal media only (no factors), addition of all 3 factors (ALK5i/TBP/Noggin) during S4 significantly reduced expression of nonpancreatic lineage markers in S4, including mesenchyme (HAND1), intestine (CDX2), and lung (NKX2.1) in culture (*F*) and reduced the overgrowth of cells following transplantation (*H*). *G*: Human C-peptide levels (ng/mL) at 4, 8, 12, and 16 weeks following transplantation of hESCs differentiated with or without the 3 factors in S4 media. Data in panels *A–C* are presented as mean ± SD, and data in panels *D–G* are presented as mean ± SEM. (A high-quality digital representation of this figure is available in the online issue.)

addition ALK5i/Noggin/TPB). The improved in vivo outcome was achieved without further enhancing *PDX1* expression (Fig. 1*F*), but is likely a reflection of *NKX6.1* induction, combined with inhibition of nonpancreatic lineages (Fig. 1*F*). However, *NKX6.1* induction alone was insufficient to predict the successful development of insulin-producing cells in vivo. Removing ALK5i from the stage 4 formulation further increased the proportion of NKX6.1-positive cells in culture, but also significantly reduced the NEUROD1-positive population (Fig. 1*D*). Consequently, these cells failed to mature into insulin-producing cells by 16 weeks posttransplant (Fig. 1*E*).

Characterization of in vitro differentiation protocol. On the basis of our optimization studies, a 14-day, four-stage differentiation protocol was established to generate pancreatic endocrine precursor cells (Fig. 2*A*). Throughout the differentiation, cells expressed appropriate markers of the developing pancreatic endocrine lineage, including loss of pluripotency markers (Fig. 2*E*), transient induction of definitive endoderm (Fig. 2*E*), and sequential induction of key pancreatic transcription factors, starting with PDX1 in stage 3 (Fig. 2*B*). High levels of pancreatic hormones were detected throughout stage 4 (Fig. 2*C*), in contrast with comparably low levels of other lineage markers (Fig. 2*D*). At stage 4 day 4 the monolayer cultures were extremely uniform, with 98% of cells expressing PDX1 and 86% expressing NKX6.1; importantly, these criteria are achieved routinely in ~70% of H1 cultures within our laboratory (Fig. 2*F* and Supplementary Fig. 2). After overnight cluster formation, there was a consistent reduction in NKX6.1-positive cells and enhancement of the endocrine compartment (indicated by NKX2.2 and synaptophysin; Fig. 2*G*). Before transplantation, the suspension clusters were composed of ~50% pancreatic endocrine cells (NKX2.2 positive) and ~50% pancreatic endoderm cells (NKX6.1/PDX1 copositive) (Fig. 2*G* and *H* and Supplementary Fig. 3). The pretransplant clusters contained 12% insulin-positive and 19% glucagon-positive cells, but a large proportion of these coexpressed both insulin and glucagon (Fig. 2*G* and *H*; quantified in Fig. 4*E*). The majority of insulin-positive cells before transplant did not express β-cell transcription factors, such as PDX1 or NKX6.1. Glucagon-positive and bihormonal cells expressed ARX, and the majority of synaptophysin-positive cells coexpressed NKX2.2 (Fig. 2*H*).

Cell expansion was observed throughout the 14-day differentiation (Supplementary Fig. 4*B*) with a progressive decline in proliferation throughout stage 4 (Supplementary Fig. 4*A*). Similarly, ongoing proliferation was observed in both endocrine and ductal cells posttransplant, but this decreased over time such that by 8 months posttransplant there were few PCNA+ engrafted cells except in isolated regions of ductal cells (Supplementary Fig. 4*D*). Importantly, at the time of transplant stage 4 cell clusters expressed similar levels of pluripotency markers to human islets (Supplementary Fig. 4*C*).

The same differentiation protocol was also applied to ESI-49 cells to assess efficiency in another hESC line (Supplementary Fig. 5). Although the induction of pancreas hormones was less efficient in ESI-49 cells compared with H1 cells, gene expression of pancreas transcription factors was similar (Supplementary Fig. 5*A* and *B*) and the proportion of cells expressing NKX6.1 before transplant was higher (~60% in ESI-49 cells, Supplementary Fig. 5*C*; ~40% in H1 cells, Fig. 2*G*). Moreover, differentiated ESI-49 cells were capable of in vivo maturation into human C-peptide–secreting cells in a similar time frame to H1 cells (Supplementary Fig. 5*D* vs. Fig. 3*C* and *D*), although significantly larger overgrowths were observed in vivo with ESI-49 cells as compared with the H1 line (data not shown).

Tracking development of hESCs in vivo. Stage 4 day 4 hESC-derived clusters were transplanted under the kidney capsule of diabetic (STZ-injected) or nondiabetic mice. At the time of transplant all STZ-injected mice exhibited severe hyperglycemia that was subsequently treated with slow-release insulin pellets (Fig. 3*A* and *B*; red arrows). Insulin pellets were replaced monthly for the first 3 to 4 months, as the immature engrafted cells developed in vivo (Fig. 3*A* and *B*). After this time mice in both cohorts maintained glucose levels that were similar to nondiabetic (no STZ) control mice, without requiring an additional insulin pellet implant. Therefore, mice were maintained without exogenous insulin for an additional 2.5–4 months until the studies were terminated (Fig. 3*A* and *B*).

To monitor the development of hESC-derived cells in vivo, human C-peptide was measured monthly after an overnight fast and subsequent 45-min meal. Between 12 and 16 weeks posttransplant, there was an approximately fourfold increase in circulating human C-peptide levels that coincided with the mice being weaned from exogenous insulin therapy (Fig. 3*C*). A similar increase in human C-peptide levels was also observed in nondiabetic mice (Fig. 3*D*) and nude rats (Supplementary Fig. 7). Human C-peptide levels from individual mice are provided in Supplementary Fig. 6. In both cohorts 1 and 2, meal-regulated C-peptide secretion was observed by 30 weeks posttransplant (Fig. 3*C*).

Mice were subjected to various glucose challenges to further assess the regulation of human C-peptide secretion. At 12 and 25 weeks posttransplant, engrafted cells were not glucose responsive in mice (Fig. 3*F*), but glucose tolerance improved significantly and human C-peptide levels increased ~10-fold between 12 and 25 weeks (Fig. 3*E* and *F*, insets). It is noteworthy that we observed robust glucose-stimulated human C-peptide secretion as early as 14 weeks posttransplant in the nude rat model (Supplementary Fig. 7*D*). At 32 and 34 weeks, the glucose tolerance of mice administered STZ and transplanted with hESCs was indistinguishable from nondiabetic mice with engrafted human islets (Fig. 3*G* and *I*). Furthermore, the hESC-derived cells secreted human C-peptide in a glucose-dependent manner, similar to engrafted human islets, following both intraperitoneal and oral glucose challenges (Fig. 3*H* and *J*), although hESC-derived cells secreted lower absolute levels of human C-peptide than human islets (intraperitoneal glucose tolerance test fasting: hESCs 2.89 ± 0.51 vs. human islets 5.01 ± 1.4 ng/mL; oral glucose tolerance test fasting: hESCs 2.86 ± 0.65 vs. human islets 4.43 ± 1.0 ng/mL). Despite the lower absolute levels of human C-peptide, hESCs maintained normal glucose tolerance (Fig. 3*G* and *I*) in the absence of any detectable mouse C-peptide (Supplementary Fig. 8*A*). Similarly, during meal challenges mouse C-peptide was undetectable in STZ-injected mice at 8 and 30 weeks posttransplant, whereas human C-peptide levels increased as the engrafted hESCs developed in vivo (Supplementary Fig. 8*B*). In contrast, nondiabetic mice transplanted with human islets had high circulating levels of both mouse and human C-peptide (Supplementary Fig. 8*A* and *B*). Endogenous pancreatic β-cell area in mice given STZ was ~10% that of healthy control mice and did not change between 3 and 8 months post-STZ administration (Supplementary Fig. 8*C*–*F*). These

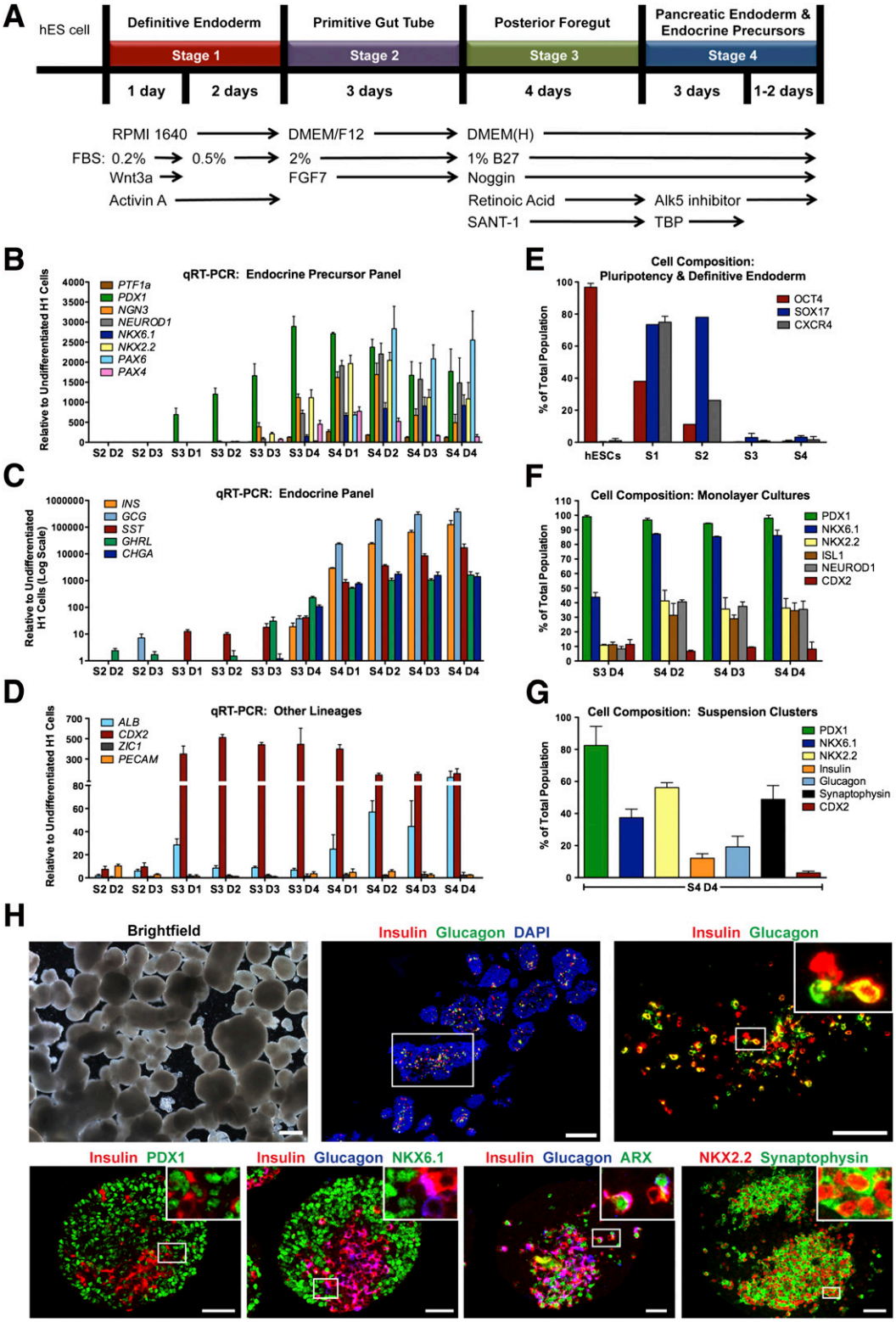

FIG. 2. Characterization of hESC-derived pancreatic progenitor cells before transplantation. *A*: Schematic of the 14-day, 4-stage differentiation protocol. Gene expression was assessed throughout stages 2–4 (S2–S4) and expressed relative to undifferentiated H1 cells for levels of endocrine precursor markers (linear scale) (*B*), pancreatic hormones (log scale) (*C*), and other lineages, including hepatic (*ALB*), intestinal (*CDX2*), neural crest (*ZIC1*), and hematopoietic (*PECAM*) (*D*). *E*: Fluorescence-activated cell sorter (FACS) quantification of the proportion of cells expressing OCT4, SOX17, or CXCR4 during each stage of in vitro development. *F*: Quantification of various pancreatic and intestinal lineage markers in monolayer cultures by high content imaging from stage 3 day (D) 4 to S4 D4. *G*: FACS quantification of the proportion of cells expressing various transcription factors, insulin, glucagon, and synaptophysin in S4 suspension cell clusters before transplantation. *H*: Representative images of cell clusters before transplant, including brightfield (scale bar = 500 μm) and immunofluorescent staining for insulin, glucagon, synaptophysin, and various transcription factors (scale bars = 50 μm). All data are presented as mean ± SD. qRT-PCR, quantitative RT-PCR; hES, human embryonic stem. (A high-quality digital representation of this figure is available in the online issue.)

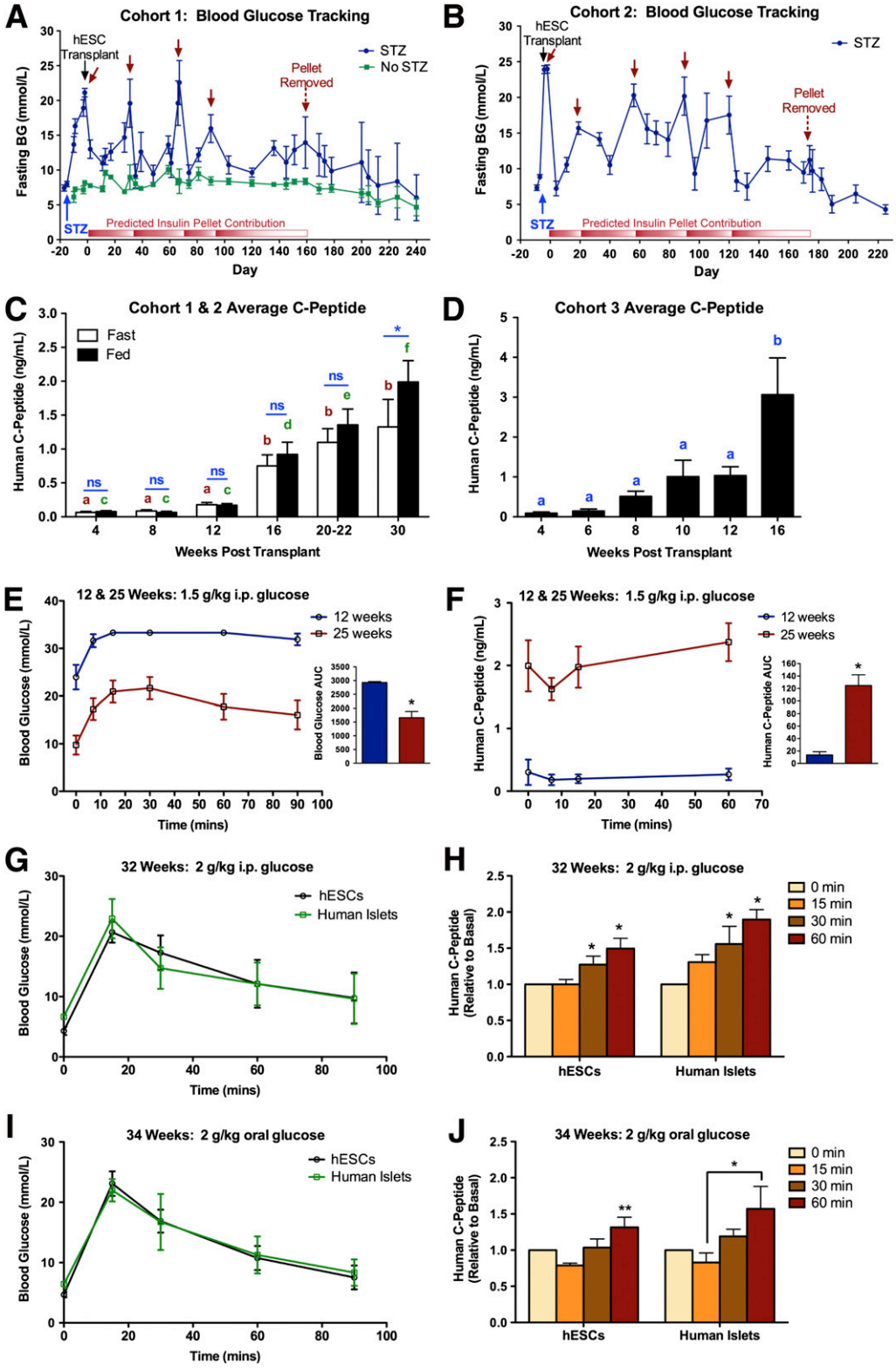

FIG. 3. In vivo tracking of pancreatic endocrine progenitor cells following transplantation. *A* and *B*: Blood glucose (BG) levels (mM) following a 4-h fast in mice with (blue) and without (green) STZ for up to 240 days following transplant. A slow-release insulin pellet was replaced as needed (red arrows). Red bars represent the predicted duration of insulin pellet contribution to glucose homeostasis; white regions indicate periods of time when there was likely no contribution from the implanted insulin pellet. By 21 weeks, mice in two cohorts were normoglycemic without exogenous insulin. *C*: Average human C-peptide levels (ng/mL) after an overnight fast and a 45-min meal at various time points posttransplant in cohorts 1 and 2. C-peptide levels increased over time (fasted: a vs. b = $P < 0.05$, fed: c vs. d/e/f, d vs. e/f, and e vs. f = $P < 0.05$). At 30 weeks, engrafted cells secreted human C-peptide in response to the meal challenge (*$P < 0.05$, fed vs. fast; ns, not significant). *D*: Average human C-peptide levels in random fed plasma samples from cohort 3 (a vs. b = $P < 0.05$). Blood glucose (*E*) and human C-peptide levels (*F*) after a 1.5 g/kg i.p. glucose tolerance test (GTT) at 12 and 25 weeks posttransplant are shown. Area under the curve (AUC) values are provided in the inset bar graphs (*$P < 0.05$, 12 vs. 25 weeks). *G* and *I*: STZ-injected mice with engrafted hESCs (black lines) had normal glucose tolerance, comparable with nondiabetic (no STZ; green lines) mice transplanted with human islets, during an intraperitoneal (*G*) and oral (*I*) GTT at 32 and 34 weeks posttransplant, respectively. *H* and *J*: Human C-peptide was secreted from hESC-derived cells in a similar manner to engrafted human islets during both the intraperitoneal (*H*; *$P < 0.05$, vs. 0 min) and oral (*J*; *$P < 0.05$, 60 vs. 15 min; **$P < 0.05$, 60 vs. 0, 15, and 30 min) GTTs. All values are provided as mean ± SEM.

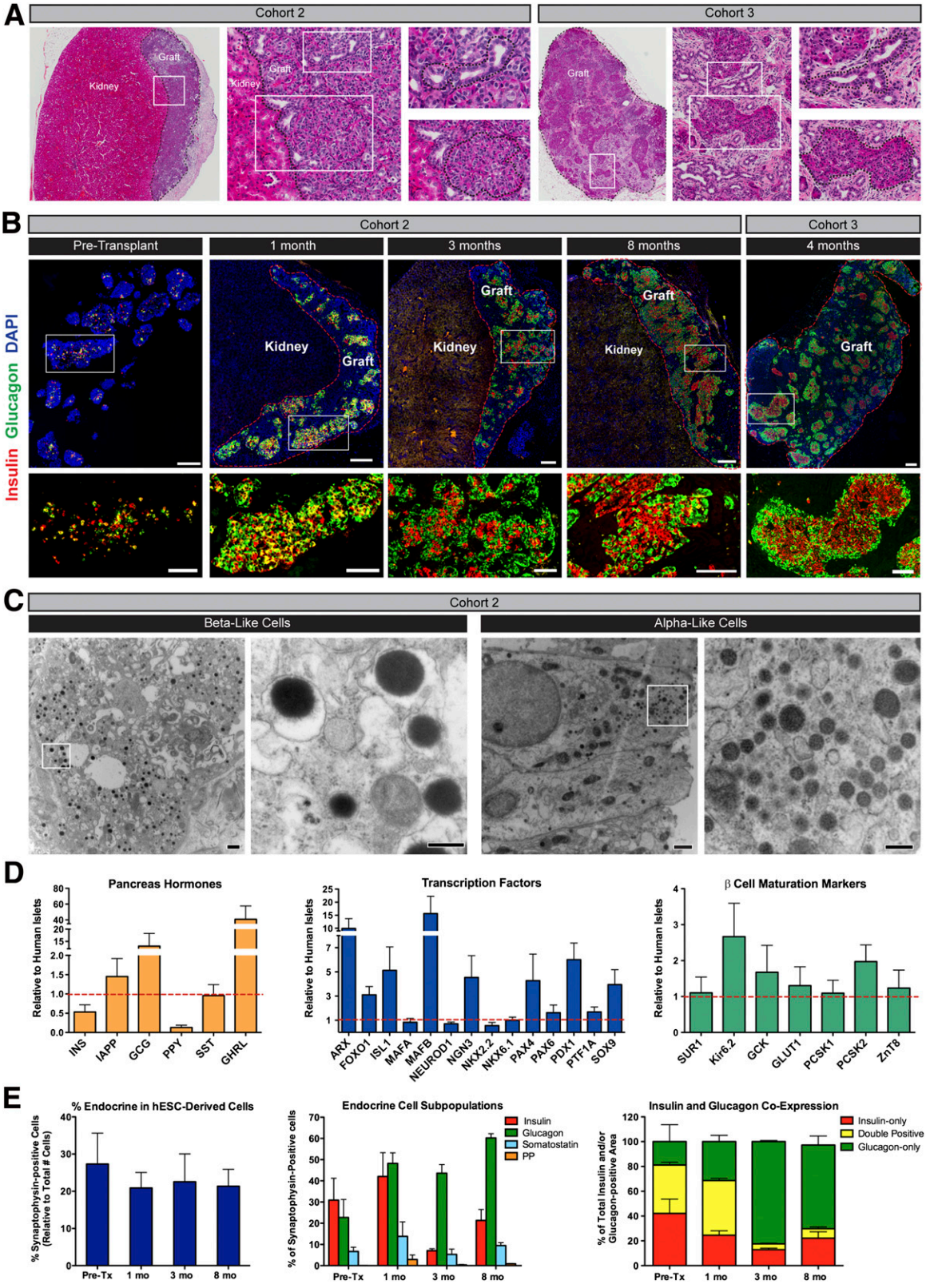

FIG. 4. Graft morphology and composition after transplantation. *A*: Representative image of Hematoxylin-eosin (H&E)–stained kidney with engrafted hESC-derived cells at 34 weeks posttransplant from cohort 2 and dissected graft tissue at 17 weeks from cohort 3. Enlarged regions show examples of ductal (top) and islet-like (bottom) structures, outlined in dashed black lines. *B*: Representative images of insulin (red) and glucagon (green) expression in hESC-derived cells from cohort 2 before and at 1, 3, and 8 months after transplantation, and cohort 3 at 4 months. Engrafted tissue is demarcated from the kidney by red dashed lines, and enlarged regions illustrating endocrine expression patterns are shown below (without DAPI). Insulin/glucagon bihormonal cells (yellow) were observed pretransplant and at 1 month posttransplant (see inset images; quantified in panel *E*). Scale bars in top panel = 200 μm and bottom panel = 50 μm. *C*: Transmission electron microscopy images of engrafted endocrine cells that resemble pancreatic β-like cells (left) and α-like cells (right), containing insulin- and glucagon-like granules, respectively. Scale bars for low-magnification images = 2 μm and high-magnification images = 500 nm. *D*: Gene expression of pancreas hormones, islet

data indicate that the glucose control in STZ-injected mice (Fig. 3*A* and *B*) was attributed to increasing levels of graft-derived insulin and not to recovery of endogenous β-cell mass.

Immunohistochemical and subcellular characterization of graft development in vivo. To further characterize the development of hESC-derived cells in vivo, engrafted kidneys were examined at 1, 3, and 8 months posttransplant from mouse cohort 2 (Figs. 4–8). End-stage engrafted cells from cohort 3 are shown to illustrate reproducibility. Hematoxylin-eosin–stained kidney grafts show the presence of islet-like cell clusters and ductal structures within engrafted tissue, a finding that was confirmed by an independent pathologist (Fig. 4*A*). However, in a subset of mice the presence of mature bone and cartilage was also detected in grafts at 8 months posttransplant (Supplementary Table 1 and Supplementary Fig. 9). With the exception of sporadic mesoderm formation, the in vivo development of hESC-derived cells was remarkably similar to human fetal pancreas development.

Before transplant, hESC-derived cells expressing insulin and/or glucagon were scattered and disorganized; ~40% of the endocrine cells at this time coexpressed both insulin and glucagon (Fig. 4*B* and *E*). After 1 month in vivo, the endocrine population was similar, although distinct islet-like clusters had formed (Fig. 4*B*). By 3 months, ~95% of endocrine cells were single hormone positive, and this morphology was maintained until the end point the studies (Fig. 4*B* and *E*). Similarly, monohormonal insulin-, glucagon-, and somatostatin-positive cells were also observed in grafts retrieved from nude rats (Supplementary Fig. 7*E*). TEM confirmed the presence of endocrine granules in engrafted cells that resembled the ultrastructural morphology of insulin and glucagon granules (Fig. 4*C*). Although the proportion of endocrine cells within the hESC-derived tissue did not change over time, the relative endocrine cell subpopulations varied (Fig. 4*E*). Initially, there were relatively equal proportions of insulin and glucagon-expressing cells within the endocrine compartment, but by 3 months posttransplant, glucagon-positive cells outnumbered the insulin-positive population (Fig. 4*E*); quantitative PCR confirmed that hESC-derived cells expressed ~10-fold higher levels of glucagon and *ARX* relative to human islets (Fig. 4*D*). Although insulin gene expression was lower in hESC-derived tissue from mice compared with human islets, key β-cell transcription factors and markers of mature β-cells (*SUR1*, *KIR6.2*, glucokinase, *GLUT1*, prohormone processing enzymes, and *ZNT8*) were expressed at similar or higher levels (Fig. 4*D*). Furthermore, the architecture of insulin and glucagon-positive clusters of hESC-derived cells closely resembled mature human islets (Fig. 5*A* and *D*) and similarly contained other pancreatic hormones, such as somatostatin and pancreatic polypeptide (Fig. 5*B* and *C*). Unlike adult human pancreas, which contains majority amylase- and trypsin-positive exocrine cells, the hESC-derived tissue contained mainly endocrine cells surrounded by a network of CK19/PDX1 copositive ductal cells (Fig. 6*A*–*C*). However, although there were virtually no detectable amylase-positive cells in the engrafted tissue (Fig. 6*A*), small regions of trypsin-positive cells were evident in the hESC-derived grafts (Fig. 6*B*). As in human pancreas, the ductal cells expressed low levels of PDX1, whereas the insulin-positive cells strongly expressed PDX1 (Fig. 6*C*).

We next assessed expression of key pancreatic islet transcription factors in the engrafted insulin- and/or glucagon-positive cells throughout development. PDX1 and NKX6.1 were abundant in cells surrounding the endocrine population before transplant (Fig. 2*H*, Supplementary Fig. 3) and at 1 month posttransplant (Fig. 7*A* and *B*). At these early stages, PDX1 and NKX6.1 were expressed in only rare insulin-positive cells, but later became restricted to the insulin-positive population and were never observed in the copositive or glucagon-positive cells (Fig. 7*A* and *B*). In contrast, ARX was expressed in both copositive and glucagon-only cells at 1 month and became mainly restricted to the glucagon-positive population at later stages (Fig. 7*C*). NKX2.2 and MAFB were expressed in insulin-only, glucagon-only, and copositive cells throughout development (Fig. 7*D* and *F*), whereas MAFA was only expressed in insulin-positive cells, but not until later stages of development (Fig. 7*E*).

To further assess if the hESC-derived insulin-positive cells resembled adult β-cells, we examined key markers of functional, mature β-cells. In general, these markers were sporadically expressed at 1 and 3 months posttransplant, but by 8 months, the insulin-positive population consistently possessed characteristics of mature β-cells (Fig. 8), confirming the gene expression findings (Fig. 4*D*). For instance, insulin-positive cells expressed the appropriate prohormone convertase enzymes required for insulin processing, PC1/3 and PC2 (Fig. 8*A* and *B*), and C-peptide was detected in all insulin-positive cells (Fig. 8*C*). Islet amyloid polypeptide, known to be cosecreted with insulin, was not expressed at 1 month and only sporadically at 3 months, but was highly expressed in the majority of insulin-positive cells at later stages (Fig. 8*D*). ZNT8 was strongly expressed in insulin-positive cells and weakly in glucagon-positive cells at all ages examined and was also present in the copositive cells at 1 month (Fig. 8*E*).

DISCUSSION

In these studies, we have optimized a 4-stage protocol for differentiating pluripotent hESCs into a highly enriched PDX1+ pancreatic endoderm population in vitro without cell sorting. The development of these progenitor cells in vivo was remarkably similar to human fetal pancreas development and resulted in the formation of insulin-producing cells that closely resembled mature human β-cells. At the time of transplant, hESC-derived cells were composed of mainly immature polyhormonal cells and pancreatic progenitor cells and, thus, insufficient for treating hyperglycemia. Therefore, diabetic mice were administered

transcription factors, and β-cell maturation markers in engrafted cells at 8 months posttransplant relative to human islets (red dashed line indicates the level of expression in adult human islets). *E*: Quantification of the endocrine compartment in immunofluorescent images of pretransplant clusters and engrafted cells at 1, 3, and 8 months posttransplant under the kidney capsule. The proportion of endocrine cells within the hESC-derived tissue (number of synaptophysin-positive cells/total number of hESC-derived cells) was determined, as well as the relative number of endocrine cells expressing each of the four main pancreatic hormones (number of synaptophysin-positive cells that coexpress insulin, glucagon, somatostatin, or pancreatic polypeptide/total number of synaptophysin-positive cells). Insulin and glucagon coexpression was assessed as the insulin-positive, glucagon-positive, or insulin/glucagon copositive area relative to the total insulin and/or glucagon-positive area. Data are presented as mean ± SEM. (A high-quality digital representation of this figure is available in the online issue.)

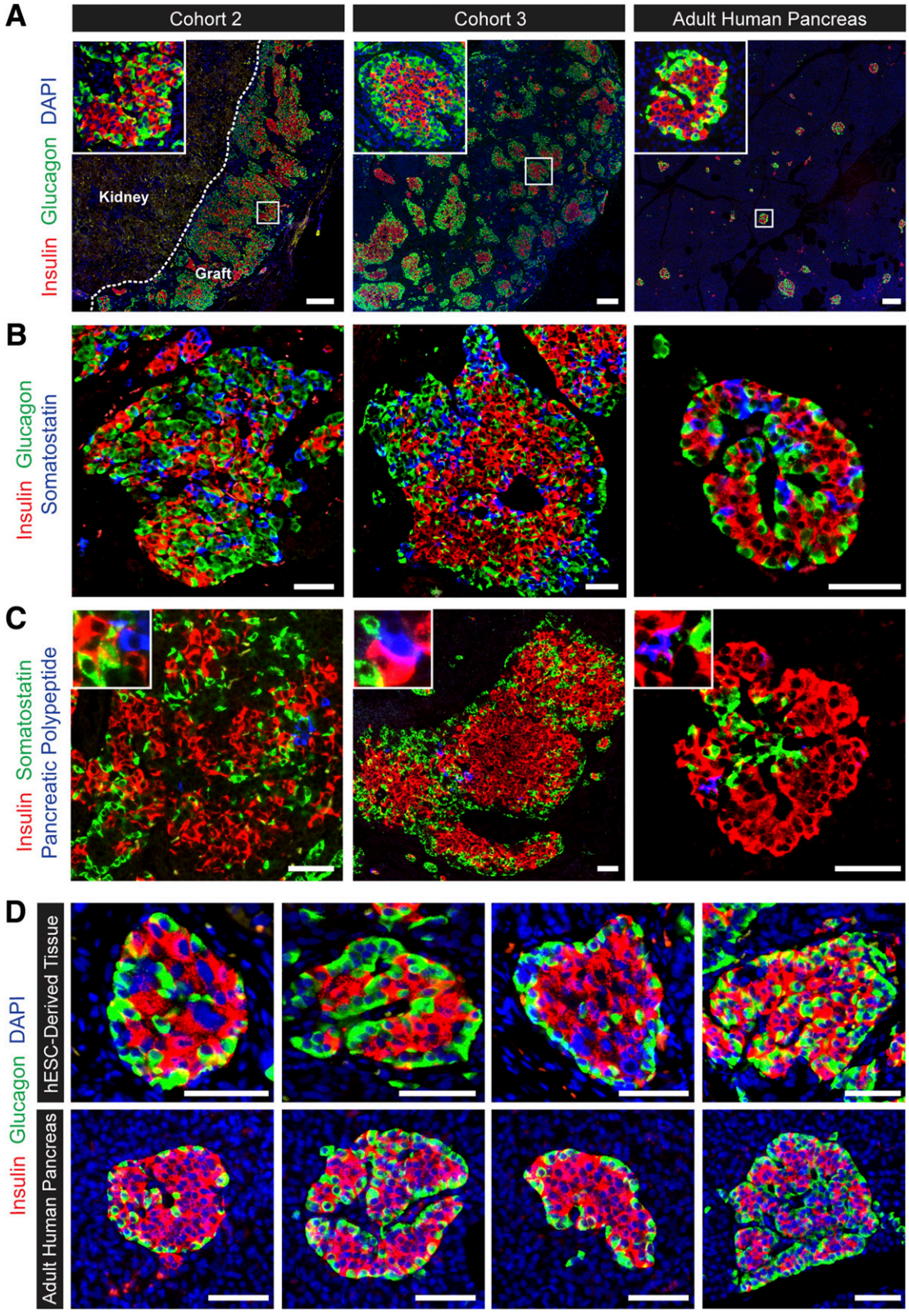

FIG. 5. Comparison of islet-like endocrine cells in mature hESC-derived and adult human pancreas. *A–C*: Representative immunofluorescent staining of hESC-derived engrafted cells from cohorts 2 (34 weeks) and 3 (17 weeks), as compared with adult human pancreas. *A*: The distribution of insulin and glucagon expression in engrafted hESC-derived cells versus adult human pancreas. Scale bars = 200 μm. Islet-like endocrine clusters also express other pancreatic hormones, including somatostatin (*B*) and pancreatic polypeptide (*C*) (see insets); scale bars = 50 μm. *D*: Various examples of observed islet-like architecture within hESC-derived engrafted cells at 8 months posttransplant (top row), closely resembling the typical islet morphologies observed in adult human pancreas (bottom row). Scale bars = 50 μm. (A high-quality digital representation of this figure is available in the online issue.)

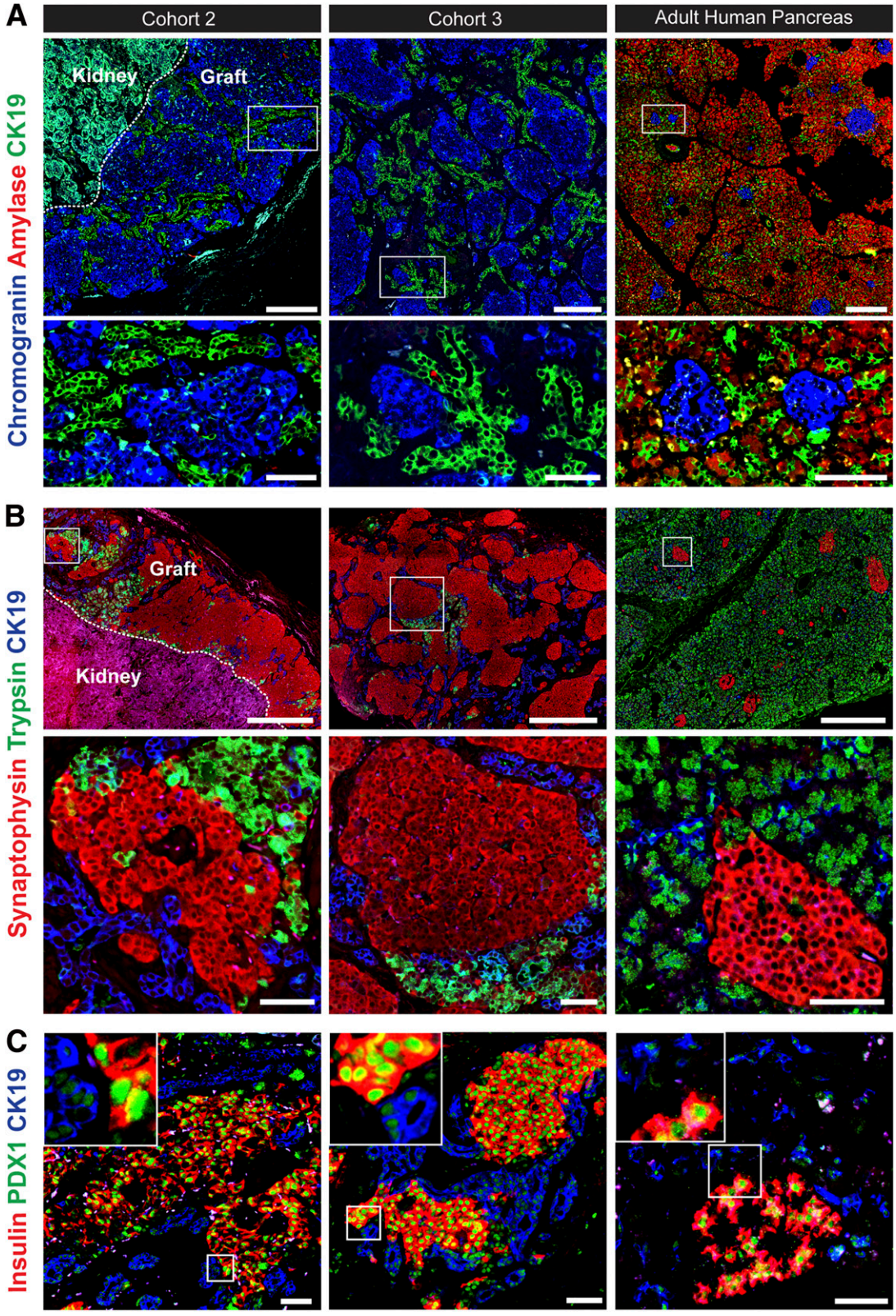

FIG. 6. Comparison of endocrine, exocrine, and ductal compartments in mature hESC-derived engrafted tissue and adult human pancreas. *A*: hESC-derived engrafted cells were composed mainly of endocrine (chromogranin A-positive; blue) and ductal (CK19-positive; green) cells and lacked expression of amylase, a marker of mature acinar cells (red); enlarged regions are shown below. Scale bars in top panel = 200 μm and bottom panel = 50 μm. *B*: Trypsin immunoreactivity (green) was detected in small regions of the mature, engrafted cells; enlarged regions showing the presence of endocrine (synaptophysin-positive; red), ductal (CK19-positive; blue), and immature exocrine (trypsin-positive; green) cells are shown below. Scale bars in top panel = 500 μm and bottom panel = 50 μm. *C*: PDX1 (green) was weakly expressed in CK19-positive ductal cells (blue) and strongly expressed in neighboring insulin-positive cells (red), similar to adult human pancreas; scale bars = 50 μm. (A high-quality digital representation of this figure is available in the online issue.)

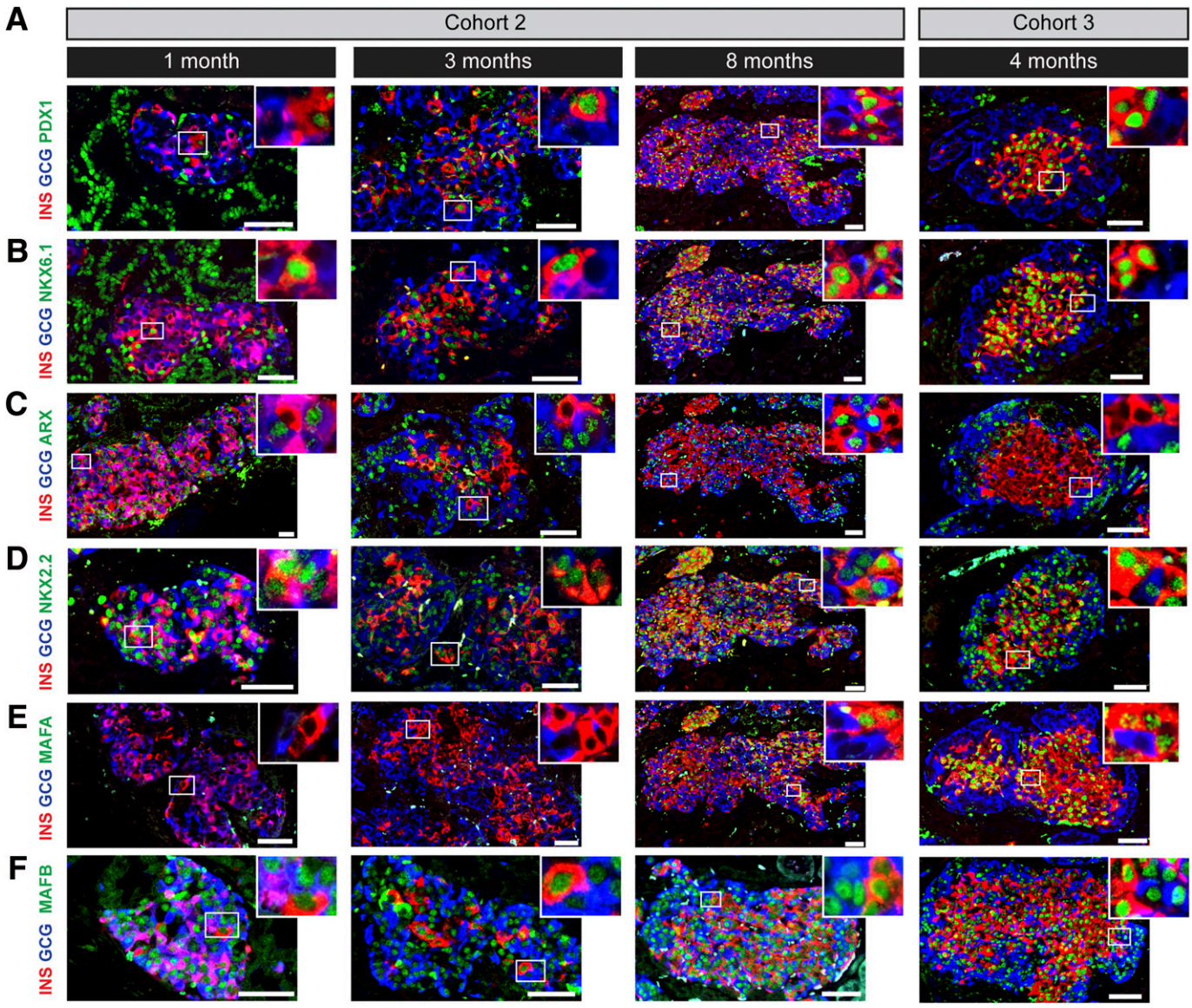

FIG. 7. Transcription factor expression in insulin- and glucagon-positive cells during graft maturation. hESC-derived cells from cohort 2 at 1, 3, and 8 months posttransplant, and cohort 3 at 4 months, immunostained for insulin (INS; red), glucagon (GCG; blue), and various transcription factors (green), including PDX1 (*A*), NKX6.1 (*B*), ARX (*C*), NKX2.2 (*D*), MAFA (*E*), and MAFB (*F*). See insets for an enlarged region illustrating transcription factor localization. All scale bars = 50 μm. (A high-quality digital representation of this figure is available in the online issue.)

exogenous insulin until the engrafted cells produced sufficient insulin to achieve normoglycemia. After 30 weeks in vivo, hESC-derived cells secreted appropriately regulated human C-peptide in response to meal and glucose challenges.

These studies are the first to externally reproduce important aspects of previous work by ViaCyte (4,10), including the generation of human glucose-responsive insulin-secreting cells in vivo that express key β-cell maturity markers. We have also demonstrated several key advancements that are particularly relevant from a clinical cell therapy perspective. Our modifications to the differentiation protocol enhanced production of pancreatic progenitor cells, while minimizing other nonpancreatic lineages and preventing overgrowth of fluid-filled cysts following transplant. Further work is required to understand why sporadic mesoderm formation still occurs in ~50% of the mice following transplant, even though the presence of focal bone/cartilage tissue in the grafts did not seem to affect pancreatic endocrine function. Our protocol was adapted for a commercially available hESC line so that it can be widely reproduced. We also demonstrated that this protocol could be applied to ESI-49 cells, but differentiation conditions will likely need optimization for individual cell lines to account for their inherent variability (8,9,11,20). Next, we validated the capacity of pancreatic progenitors to mature within a diabetic environment into functional insulin-producing cells, an important advance over previous work that had demonstrated maturation in healthy, nondiabetic mice (4,10). Our studies were designed to mimic a clinical scenario, in which a diabetic patient could feasibly titer insulin therapy while the transplanted cells developed into the primary source of insulin. We also confirmed that hESC-derived progenitor cells could mature in a second animal model, immunocompromised nude rats. Finally, unlike previous studies that focused on

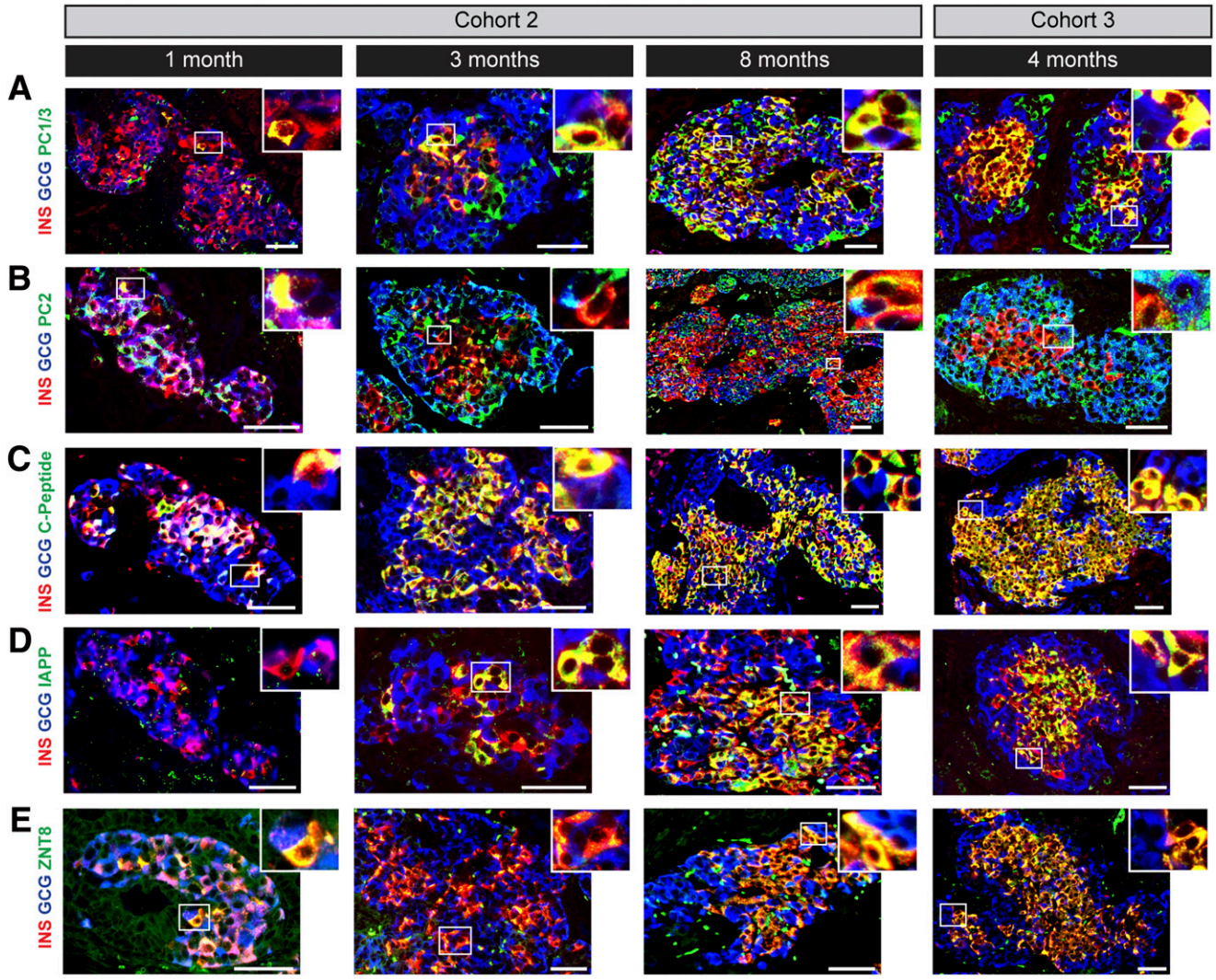

FIG. 8. Characteristics of mature β-cells. hESC-derived cells from cohort 2 at 1, 3, and 8 months posttransplant, and cohort 3 at 4 months, immunostained for insulin (INS; red), glucagon (GCG; blue), and various markers of mature β-cells (green), including prohormone convertase 1/3 (PC1/3) (*A*), PC2 (*B*), C-peptide (*C*), islet amyloid polypeptide (IAPP) (*D*), and zinc transporter 8 (ZNT8) (*E*). See insets for an enlarged region illustrating marker colocalization with insulin-positive cells. All scale bars = 50 μm. (A high-quality digital representation of this figure is available in the online issue.)

characterizing only the mature end-stage cells following transplantation (4,6,10,12), we assessed our cells throughout their in vivo development to gain further insights into the maturation process.

We believe that the combined differentiation of hESCs in vitro and in vivo closely parallels human fetal pancreas development, in terms of timing and patterns of gene/protein expression, as well as tissue morphology and function (27). For instance, as in human fetal pancreas (27–29), PDX1 and NKX6.1 were widely expressed throughout the hESC-derived epithelium at early stages of development and later became restricted to insulin-positive cells. The transition from scattered endocrine cells before transplant into distinct islet-like clusters after 1 month in vivo resembled the formation of human fetal islets by 12–14 weeks postconception (27–29). The hESC-derived insulin/glucagon coexpressing cells were also remarkably similar to the bihormonal cells observed during human fetal pancreas development, both in their transient nature and transcription factor expression profile (negative for PDX1, NKX6.1, and MAFA; positive for ARX, MAFB, and NKX2.2 [27]). Notably, hESC-derived insulin-positive cells progressively acquired mature β-cell characteristics throughout development, such as MAFA expression and meal/glucose-regulated insulin secretion. This also paralleled the human fetal pancreas, which develops glucose responsiveness after 25 weeks of gestation (30).

There were several key findings from our in vitro optimization studies that contributed to the successful in vivo outcomes. We determined that DMEM-HG medium was optimal for promoting formation of the pancreatic lineage in H1 cells and this may be mediated, in part, by the absence of HEPES buffer. Others recently demonstrated that basal media components can affect pancreatic gene expression (31); the underlying reason for the HEPES-mediated effect in our differentiation protocol is currently unknown. The endocrine progenitor population was dramatically enhanced by the addition of Noggin, ALK5i, and TPB in stage 4 media. We had previously reported that the combined inhibition of transforming growth factor-β and bone morphogenetic protein signaling with ALK5i and

Noggin, respectively, during stage 4 induced endocrine formation (18), and the importance of bone morphogenetic protein inhibition was recently confirmed (8,32). The current study demonstrated that the addition of a PKC activator (TPB) at stage 4 further enhanced the development of pancreatic progenitors, while minimizing the formation of intestinal and hepatic lineages, confirming a previous report (25). It is noteworthy that without all three stage 4 factors, transplanted cells secreted high levels of human C-peptide in vivo, but also formed overgrown grafts containing fluid-filled cysts. Although we did observe graft expansion following transplantation of pancreatic progenitor cells in our studies, this was comparable with the observed expansion of engrafted healthy human fetal pancreas tissue under the kidney capsule of SCID mice (33).

These studies demonstrate that hESCs can differentiate in vivo into insulin-producing cells with the capacity to treat pre-existing STZ-induced diabetes. The development of hESCs closely mimicked human fetal pancreas development, and, as such, insulin-positive cells did not develop characteristics of mature β-cells until several months posttransplant. Notably, this maturation process was achieved in a clinically relevant diabetic setting in the presence of exogenous insulin until engrafted cells produced sufficient levels of human insulin to independently control hyperglycemia. Further optimization and testing of both safety and efficacy of this approach as a therapy for diabetes are warranted, in combination with efforts to contain transplanted cells and isolate them from immune attack.

ACKNOWLEDGMENTS

This work was funded by the Canadian Institutes of Health Research (CIHR) Regenerative Medicine and Nanomedicine Initiative, the Stem Cell Network (SCN), Stem Cell Technologies, and the Juvenile Diabetes Research Foundation (JDRF). T.J.K. was supported by a senior scholarship from the Michael Smith Foundation for Health Research. J.E.B. and M.M. were both funded by JDRF postdoctoral fellowships, as well as the CIHR Transplantation Training Program. J.E.B. was also funded by a CIHR postdoctoral fellowship. M.J.R. was supported by the SCN. A.R., J.X., R.G., K.N., F.K., and J.J.O. are employees of Janssen R&D, LLC, and T.J.K. received financial support from Janssen R&D, LLC, for the research described in this article. No other potential conflicts of interest relevant to this article were reported.

J.E.B. wrote the first draft of the manuscript. A.R., J.E.B., M.J.R., M.M., A.A., F.K., and T.J.K. contributed to manuscript edits and revisions. A.R., J.E.B., M.J.R., F.K., and T.J.K. designed, directed, and interpreted experiments. A.R., J.E.B., M.J.R., M.M., A.A., J.X., R.G., K.N., F.K., and J.J.O. performed experiments. Human islets were provided by Z.A. and G.L.W. T.J.K. is the guarantor of this work and, as such, had full access to all the data in the study and takes responsibility for the integrity of the data and the accuracy of the data analysis.

The authors thank Madeleine Speck and Travis Webber of the University of British Columbia for their technical assistance with various aspects of these studies.

REFERENCES

1. Mathis D, Vence L, Benoist C. Beta-cell death during progression to diabetes. Nature 2001;414:792–798
2. Ryan EA, Lakey JR, Rajotte RV, et al. Clinical outcomes and insulin secretion after islet transplantation with the Edmonton protocol. Diabetes 2001;50:710–719
3. Shapiro AM, Lakey JR, Ryan EA, et al. Islet transplantation in seven patients with type 1 diabetes mellitus using a glucocorticoid-free immunosuppressive regimen. N Engl J Med 2000;343:230–238
4. Kelly OG, Chan MY, Martinson LA, et al. Cell-surface markers for the isolation of pancreatic cell types derived from human embryonic stem cells. Nat Biotechnol 2011;29:750–756
5. Jiang J, Au M, Lu K, et al. Generation of insulin-producing islet-like clusters from human embryonic stem cells. Stem Cells 2007;25:1940–1953
6. Jiang W, Shi Y, Zhao D, et al. In vitro derivation of functional insulin-producing cells from human embryonic stem cells. Cell Res 2007;17:333–344
7. Zhang D, Jiang W, Liu M, et al. Highly efficient differentiation of human ES cells and iPS cells into mature pancreatic insulin-producing cells. Cell Res 2009;19:429–438
8. Nostro MC, Sarangi F, Ogawa S, et al. Stage-specific signaling through TGFβ family members and WNT regulates patterning and pancreatic specification of human pluripotent stem cells. Development 2011;138:861–871
9. D'Amour KA, Bang AG, Eliazer S, et al. Production of pancreatic hormone-expressing endocrine cells from human embryonic stem cells. Nat Biotechnol 2006;24:1392–1401
10. Kroon E, Martinson LA, Kadoya K, et al. Pancreatic endoderm derived from human embryonic stem cells generates glucose-responsive insulin-secreting cells in vivo. Nat Biotechnol 2008;26:443–452
11. Mfopou JK, Chen B, Mateizel I, Sermon K, Bouwens L. Noggin, retinoids, and fibroblast growth factor regulate hepatic or pancreatic fate of human embryonic stem cells. Gastroenterology 2010;138:2233–2245.
12. Shim JH, Kim SE, Woo DH, et al. Directed differentiation of human embryonic stem cells towards a pancreatic cell fate. Diabetologia 2007;50:1228–1238
13. Cai J, Yu C, Liu Y, et al. Generation of homogeneous PDX1$^+$ pancreatic progenitors from human ES cell-derived endoderm cells. J Mol Cell Biol 2010;2:50–60
14. Gu G, Brown JR, Melton DA. Direct lineage tracing reveals the ontogeny of pancreatic cell fates during mouse embryogenesis. Mech Dev 2003;120:35–43
15. Zorn AM, Wells JM. Molecular basis of vertebrate endoderm development. Int Rev Cytol 2007;259:49–111
16. Slack JM. Developmental biology of the pancreas. Development 1995;121:1569–1580
17. Wandzioch E, Zaret KS. Dynamic signaling network for the specification of embryonic pancreas and liver progenitors. Science 2009;324:1707–1710
18. Rezania A, Riedel MJ, Wideman RD, et al. Production of functional glucagon-secreting α-cells from human embryonic stem cells. Diabetes 2011;60:239–247
19. Hayek A, Beattie GM. Experimental transplantation of human fetal and adult pancreatic islets. J Clin Endocrinol Metab 1997;82:2471–2475
20. Osafune K, Caron L, Borowiak M, et al. Marked differences in differentiation propensity among human embryonic stem cell lines. Nat Biotechnol 2008;26:313–315
21. Matveyenko AV, Georgia S, Bhushan A, Butler PC. Inconsistent formation and nonfunction of insulin-positive cells from pancreatic endoderm derived from human embryonic stem cells in athymic nude rats. Am J Physiol Endocrinol Metab 2010;299:E713–E720
22. Scott CT, McCormick JB, Owen-Smith J. And then there were two: use of hESC lines. Nat Biotechnol 2009;27:696–697
23. Crook JM, Peura TT, Kravets L, et al. The generation of six clinical-grade human embryonic stem cell lines. Cell Stem Cell 2007;1:490–494
24. Bruin JE, Gerstein HC, Morrison KM, Holloway AC. Increased pancreatic beta-cell apoptosis following fetal and neonatal exposure to nicotine is mediated via the mitochondria. Toxicol Sci 2008;103:362–370
25. Chen S, Borowiak M, Fox JL, et al. A small molecule that directs differentiation of human ESCs into the pancreatic lineage. Nat Chem Biol 2009;5:258–265
26. Kozikowski AP, Nowak I, Petukhov PA, et al. New amide-bearing benzolactam-based protein kinase C modulators induce enhanced secretion of the amyloid precursor protein metabolite sAPPalpha. J Med Chem 2003;46:364–373
27. Riedel MJ, Asadi A, Wang R, Ao Z, Warnock GL, Kieffer TJ. Immunohistochemical characterization of insulin/glucagon co-expressing cells in the developing human pancreas. Diabetologia 2012;55:372–381.
28. Jeon J, Correa-Medina M, Ricordi C, Edlund H, Diez JA. Endocrine cell clustering during human pancreas development. J Histochem Cytochem 2009;57:811–824

29. Piper K, Brickwood S, Turnpenny LW, et al. Beta cell differentiation during early human pancreas development. J Endocrinol 2004;181: 11–23
30. Hayek A, Beattie GM. Processing, storage and experimental transplantation of human fetal pancreatic cells. Ann Transplant 1997;2:46–54
31. Rachdi L, Aïello V, Duvillié B, Scharfmann R. L-leucine alters pancreatic β-cell differentiation and function via the mTor signaling pathway. Diabetes 2012;61:409–417
32. Chung WS, Andersson O, Row R, Kimelman D, Stainier DY. Suppression of Alk8-mediated Bmp signaling cell-autonomously induces pancreatic beta-cells in zebrafish. Proc Natl Acad Sci USA 2010;107: 1142–1147
33. Castaing M, Péault B, Basmaciogullari A, Casal I, Czernichow P, Scharfmann R. Blood glucose normalization upon transplantation of human embryonic pancreas into beta-cell-deficient SCID mice. Diabetologia 2001;44:2066–2076